International J. of Engg. Research & Indu. Appls. (IJERIA).
ISSN 0974-1518, Vol.9, No. II (August 2016), pp. 35-57

INTEGRATION REMOTE SENSING DATA AND HYDROLOGICAL MODELING IN STUDY IMPACT LAND COVER ON RUNOFF AND PEAK FLOOD DISCHARGE FOR TURSAQ GALAL BASIN / IRAQ EASTERN BY USING GIS

Dr. HASSAN SWADI NJEBAN
Assistant Professor
GIS Department, Iraq.

Abstract

Rainfall runoff modeling is very important in the planning and management of available water resources in a watershed. In this paper, a SCS-based unit hydrograph has been used to simulate the surface flow. Hydrologic processes such as infiltration losses and runoff are considered in the present model. Remote sensing and GIS techniques have been used to estimate the spatial variation of the hydrological parameters, which are used as input to the model. The runoff is considered as surface flow and channel flow. the present work has been applied on the Tursaq Galal basin , Which is located in eastern Iraq, which is extends between Iraq and Iran, between Latitudes (33° 01' 25" -33° 50' 52") north and Longitude (45° 40' 24"- 46° 30' 56") east, and covers an area of about (2863) km2. The basin drained by the Tursaq Galal which has a total length of about (132.4) km, and empties in the Alshwooajh marsh, which represents the point of discharge for the Tursaq Galal and seasonal valleys along the south east of study area. Tursaq Galal basin is divided into two parts where the first part located in Iran, and this part supports most of the discharge of the river according to achieved runoff within the area, and the second part is located in Iraq. The complete basins have been divided into two watersheds. The runoff from sub watersheds has been routed to the watershed outlet through channel network. The developed model is capable for simulating the event based runoff in the watersheds……...

Keywords: Land use / Land cover, Landsat images, Remote sensing, GIS, Soil Conservation Service , Curve Number, Runoff.

List of symbol

GIS	Geographic Information System
LULC	Land Use Land Cover
UTM	Universal Transfers Merector
GPS	Global Positioning System
USGS	U.S. Geological Survey
OLI	Operational Land Imager
DEM	Digital elevation model
SCS	Soil Conservation Service
CN	Curve Number
AMC	Antecedent Moisture Conditions
Ia	Initial abstraction
Q	direct runoff
S	potential maximum retention
T_C	Time of concentration
Tp	Time to peak flow
Tlag	Lag time
Qp	Peak Flow
D	Duration of the excess Rainfall

1-INTRODUCTION

Remote sensing and GIS technologies are well established tools and are routinely used in applied hydrology. In conventional applications, either results from remote sensing or from GIS analyses serve as input into hydrological models. During the last few years, research has focused on the question of how to integrate both technologies with hydrological models in integrated analysis systems.

Modeling environmental phenomena usually needs some spatial information about the distribution and the types of land cover / land use (LULC) as well as soil types investigated the use of computer analysis of Landsat Satellite Multispectral Scanner data for estimating the land cover distributions needed in operating the Soil Conservation Service (SCS) models

[1]. presented the importance of remote sensing in hydrological applications such as computation of historic monthly runoff for design purposes, and real-time flood forecasting using radar rainfall measurements for which LULC is very essential[2]. In similar concepts, a simple watershed model which uses satellite data to simulate basin runoff, more recently used satellite based remote sensing technologies to estimate the spatial variation of soil parameters for the estimation of SCS Curve Number, derived the land cover spatial information from satellite remote sensing to predict sites at risk from large peak flows associated with flash flooding in arid regions [3].

2. STUDY AREA

The Tursaq Galal basin shown Figure1 is located in eastern Iraq, which is extends between Iraq and Iran, between Latitudes (33° 01' 25" -33° 50' 52") north and Longitude (45° 40' 24"- 46° 30' 56") east, and covers an area of about (2863) km2. The basin drained by the Tursaq Galal which has a total length of about (132.4) km, and empties in the Alshwooajh marsh, which represents the point of discharge for the Tursaq Galal and seasonal valleys along the south east of study area. Tursaq Galal basin is divided into two parts where the first part located in Iran, and this part supports most of the discharge of the river basin according to achieved runoff within the area. The annual average precipitation on the Galal Tursaq basin (320 mm) by metrological data to Iranian Ilam station ,and Iraqi Badra station. The annual temperature averaged 19.5 degrees Celsius, relative humidity (50%) and the total evaporation (2806.5 mm) [4, 5].

3. OBJECT BASED METHOD

The research aims to:

1. Land use/ land cover classification of Tursaq Galal basin by using remote sensing and GIS technology.
2. Study the effect of land cover& land use on runoff and peak discharge for the Tursaq Galal basin.
3. Development a hydrological model for study area using SCS curve number and unit hydrograph methods
4. Discharge forecasting at outlet.

4. MATERIALS

4.1 DATA USED

The following ancillary data are available for the present study:

1. Satellite image, Landsat-8 Operational Land Imager (OLI) images consist of nine spectral bands with a spatial resolution of 28.5 meters for Bands 1 to 7 and 9. New band 1 (ultra-blue) is useful for coastal and aerosol studies. New band 9 is useful for cirrus cloud detection. for coastal and aerosol studies. New band 9 is useful for cirrus cloud detection. The resolution for Band 8 (panchromatic) is 15 meters. Thermal bands 10 and11 are useful in providing more accurate surface temperatures and are collected at 100 meters. Approximate scene size is 170 km north-south by 183 km east-west. Path and row 167-37 scene covering the study area were selected for the analysis. This image data were acquired 03/03/2015, which is download from GLOVIS USGS website [6].
2. Digital elevation model (DEM) with resolution 30m download from website of aster GDEM [7].
3. Height resolutions Satellite Image (IKONOS) acquired in 2009 year.
4. Soil map and geological map of Iran scale1:500000 in digital format [8, 9].
5. Field work: has field visit on 3/22/2015 and noticed several classifications. Collected a number of points using the Garmin Global Positioning System (GPS) device type CSX65 numbered 47 points distributed on classifications that have been seen during the visit of the study area were recorded navigator.
6. Metrological data for stations Ilam and Badra [4,5].

4.2 Software used: GIS/ Image processing software:

1. Erdas_14
2. Arc GIS 10.2
3. Global mapper_14

5. METHODOLOGY

The methodology can be divided in to part: The first part is the modeling of the spatial variation of terrain by remote sensing and GIS methods and creates the digital database. Second part involve in analysis of digital database of the hydrological model parameters.

5.1. Landsat 8(OLI) Image Processing

The image used in this project was extracted from a Landsat 8 (OLI), scene taken over east Iraq, (path 167, row 37), acquired on April 03 2015 .Spatial resolution for this image is 28.5 meters, without band 8 represent panchromatic resolution 14.5 meter.

5.1.1. Geometric Correction

Prior to any post processing, the geometric correction of the image were first assessed. For the Landsat 8 (OLI) image, a total of eight (8) points identifiable on both the image, were used for the geometric correction. The Universal Transverse Mercator Zone 38N World Geodetic System 1984 (UTM WGS84 zone 38N) grid coordinates system by using Erdas14 .The geometric accuracy of the image is acceptable with a global Root Mean Square Error (RMSE) of 10.22 meters and average local RMSE of 10.04, which are both less than half a pixel (<14.25 m) [10,11].

5.1.2. Colure Composite image

Landsat 8 records data in twelve band different bandwidths. These bandwidths are broken down into portions of the visible, infrared, and thermal infrared regions of the electromagnetic spectrum. From these various bandwidths, a great deal of informatio about the land cover and land use can be displayed and analyzed. This composition is from the same Landsat scene shown using bands 2, 5, and 7 (displayed in BGR respectively) In this composition vegetation appears in bright green while some of the agricultural fields, still with a good portion of bare soil, are displayed in a pink color. Also, there is a considerable amount of grass land in this scene that is displayed with a combination of the green and pink colors and can be shown some compliant in the land of Iran part.

5.1.3. Radiometric correction:

The landsat-8 images were then radiometrically corrected to at-sensor radiance the standard landsat-8 image calibration formulas and constants [11,12]a fast atmospheric correction using dark-object subtraction using band minimum.

5.2. Classification LULC from the Satellite Image:

Classification is a process intended to divide the satellite image into a number of categories or groups to represent each category, including specific geographic phenomenon on the surface of the earth. The classification process depends on the nature of the area (urban or desert or mountainous, agricultural, etc.) , spatial resolution, spectral resolution and

radiometric resolution of the satellite used [11,13].

The land use is land management objective. Some land uses, such as agriculture, (characteristic land cover pattern) and Urban Land (Residential, Industrial, commercial, and transportation). These generally appear in land cover classifications. Other land uses, such as nature conservation, are not readily discriminated by a characteristic land cover pattern [14,15].

The land cover is physical surface of the earth, including various combinations of vegetation types, soils, exposed rocks, water bodies. Land cover classes can generally be discriminated by characteristic patterns using remote sensing. [14,16].

5.2.1 Supervised classification to the study area :

Supervised classification is the process of using samples of known identity (training data) to classify the unknown identity. Knowledge of data and the desired classes are required prior to the classification process and must be obtained from ground truths, aerial photos, or maps. Supervised classification is the way category leader classification of phenomena on the image based on real information to those and through the choice of ground truth phenomena take on the nature of the field . It is a sample containing Sample set number of samples of the image, a particular area of the pixel values for each phenomenon and considers all similar phenomena in terms of pixel values that represent the fields of energy emitted and reflected them in one category. Set the name of this category of what is already present on the ground and make the program class train the classifier based image processing space to complete the classification process, on samples that have been identified and then the process of conducting an assessment of the classification accuracy, and then get evaluate classification (Accuracy assessment), can be handled classified map to a new image or map of classified and make any amendments adjustments to it [17,18].

Classified the study area by using ERDAS 2014 program and has been classified section to the reality within Iraq based on the points that were taken in the field, and braved the (47) points using a GPS type Garmin then pulled the points of the device has been converted into a Ship Fail, fell on the satellite image of the study area and reached number of items nine classes taken eight points in each category.

the Second part of the study area and located within the Iranian territory has been classified

based on the height resolutions Satellite Image (IKONOS) and map of Iran to classify soils, map Iran geological scales 1:500000 and that have been obtained from the Web site of the Iranian geology and format JPAG and then was corrected by using GIS program and system WGS84, UTM projection zone 38N.

In this study ,totally nine LULC classes were established as built-up area, forest, agriculture, grassland, mixed vegetation and bare soil(Alluvial fan deposits, Sheet Alluvial fan deposit, Brown soils and Chestnut soils, Calcareous lithosols from Sulfurous and Gypsiferous).

5.2.2 Accuracy Assessment of classification:

Classification accuracy assessment is a general term for comparing the classification to geographical data that are assumed to be true to determine the accuracy of the classification process. Usually, the assumed true data are derived from ground truth. Ground truth or field survey is done in order to observe and collect information about the actual condition on the ground at a test site and determine the relationship between remotely sensed data and object to be observed. It is recommended to have a ground truth at the same time of data acquisition, or at least within the time that the environmental condition does not change, it is usually not practical to ground truth or otherwise test every pixel of a classified image, therefore a set of reference pixel is usually used, reference pixels are points on the classified image for which actual data (will be) known. The reference pixel is randomly selected [18,19].

One of the most common means of expressing classification accuracy is the preparation of classification error matrix sometimes called a contingency table or confusion matrix. Error matrices are compared on a category by category basis, the relationship between known reference data (ground truth) and the corresponding results of an automated classification. Such matrices are square, with the number of rows and columns equal to the number of categories whose classification accuracy is being assessed [17,18].

In this study ,203 polygons for landsat8 image ,were randomly selected to assess classification accuracy. Table 1 is the error matrix ,along with the overall accuracy and Kappa coefficient. The value of Kappa coefficient confined between 0 to 1 for each class the closer the value of 1 acceptable classification. The overall accuracy of classification image 94.58% and the Kappa coefficient was 0.93. Kappa is computed as[20,21]:

$$K = \frac{N\sum_{i=1}^{r} x_{ii} - \sum_{i=1}^{r} (x_{i+} \times x_{+i})}{N^2 - \sum_{i=1}^{r} (x_{i+} \times x_{+i})}$$

Where:

N: is the total number of sites in the matrix.

r: is the number of rows in the matrix.

x_{ii} : is the number in row i and column i.

x_{+i} : is the total for row i.

x_{i+} : is the total for column i.

6. HYDROLOGIC MODELING

6.1. Digital Elevation Models (DEM) Processing

Was loaded DEM of the study area of the Website of Aster GDEM, (http://gdem.ersdac.jspacesystems.or.jp/search.jsp) and to cover the study area has been loaded, can be show in the figure (2-1) four blocks resolution 30m and accuracy were then combined and processed using the Global mapper v.14 after the merger is full of data undefined values similar to the values of pixels approach and cells are equal and interpolate the small gaps in data during mosaic by using tools for global mapper show figure (2-2) .

use geographic information system program(ArcGIS10.2) as a comprehensive modeling system for drainage basins in study area , Where the program exploits the superior ability of GIS to provide the user with the necessary tools for all aspects of modeling the drainage basin , So comprehensive Automated Delineation of the basin full or partial basins, and calculating Geometric Competent for drainage basins . The program transact with various kinds of data such as digital elevation models (DEM) Triangulated Irregular (TINs) in addition to multiple data in the retina (Raster) such as Satellite image, or in the form (Vector) such as maps. Or layers of shape file. Where the software will doing several operations main of the adoption of the analysis of data digital elevation models , the most important of these processes determine basins ,network streams water ,order streams , calculate the lengths and numbers of the streams and calculate regressions and the proportion of meanders [22].

6.2. Generation and transformation of runoff

Hydrologic modeling was performed using the Soil Conservation Service-Curve Number (SCS-CN) model [23]. The SCS-CN model, also called the runoff curve number method, for the estimation of direct runoff from storm rainfall is a well-established Method in hydrologic engineering and environmental impact analyses and has been very popular because of its convenience, simplicity, authoritative origins, and its responsiveness to four readily grasped watershed properties: soil type, land-use/land-cover and treatment, surface condition, and antecedent moisture condition [24]. The popular form of the SCS-CN model is:

$$Q = \frac{(P - I_a)^2}{P - I_a + S} \text{ for } I_a \le P, \text{ otherwise } Q = 0 \quad (1)$$

$$I_a = \lambda S \quad (2)$$

$$S = \frac{25400}{CN} - 254 \quad (3)$$

$$CN_{Composite} = \frac{(A1 + CN1) + (A2 + CN2) + (A3 + CN3)}{A1 + A2 + A3} \ldots\ldots\ldots\ldots\ldots (4)$$

Where P is total rainfall, I_a is initial abstraction, Q is direct runoff, S is potential maximum retention which can range $(0, \infty)$, and λ is initial abstraction coefficient or ratio. All variables are in millimeters (mm) except for λ which is unit less. The initial abstraction I_a includes short-term losses due to evaporation, interception, surface detention, and infiltration and its ratio to S describes λ which depends on climatic conditions and can range $(0, \infty)$. The SCS has adopted a standard value of 0.2 for the initial abstraction ratio [23] but this can be estimated through calibration with field measured hydrologic data. The potential maximum retention S characterizes the watershed's potential for abstracting and retaining storm moisture, and therefore, its direct runoff potential [24,25]. S is directly related to land-cover and soil infiltration through the parameter CN or "curve number", a non-dimensional quantity varying in the range (0–100) and depends on the antecedent moisture condition of the watershed. Higher CN values indicate high runoff potential[26]. For normal antecedent moisture conditions (AMCII, 5-day antecedent rainfall (AR) is (35.7–44.35 mm),table 2 ,the CN values for land-cover types and soil textures (hydrologic soil groups A, B,C and D)

prevalent in the study area are shown in Table 3 [27]. Spatially distributed soil texture data converted into a hydrologic soil group (HSG) map was obtained from the 1:500,000 soil map to iran and iraq.

6.3. Unit hydrograph:

Unit hydrographs were synthesized at the outlet using complete watershed as a whole as well as sub area basis. The method applied is SCS dimensionless unit hydrograph method. Followings are the parameters involve in this method[28,29].

1. Time of concentration. –T_C
2. Lag time- T_{lag}
3. Duration of the excess Rainfall-D
4. Time to peak flow-T_p
5. Peak Flow- Q_p

T_C =1.67(L)……. (5)

Where :

L= watershed lag (time from rainfall excess center of mass to peak rate of runoff) in hours watershed lag can be estimated by the formula:

$$L = \frac{e^{0.8}\,(s+1)^{0.7}}{1900\,y^{0.5}} \ldots\ldots\ldots\ldots\ldots\ldots\ldots\ldots\ldots\ldots (6)$$

Where:

e= hydraulic length of watershed, ft

Y=average watershed land slop(%)

s =SCS watershed storage parameter from the curve number method (USDA-SCS, 1985) [29].

$$\mathrm{Tp} = 0.67Tc \ldots\ldots\ldots\ldots\ldots\ldots\ldots\ldots\ldots\ldots\ldots\ldots (7)$$

Where:

Tp = Time to peak flow , T_C = Time of concentration.

The SCS peak discharge method is applicable for estimating the peak runoff from watershed with a homogeneous land use .the following method is based on

the results of computer analyses performed using TR-20(SCS 1986). The peak discharge equation is[29,31]:

$$Qp = qu\ A\ Q\ Fp \dots\dots\dots\dots\dots\dots\dots\dots\dots (8)$$

Where:

Qu= unit peak discharge, m3/s/km2/mm (cfs/mi2/in), A= drainage area km2 (mi2) Q= depth of runoff, mm (in), Fp = pond and swamp adjustment factor (If pond and swamp areas are spread throughout watershed and are not considered in the T_C computation ,and adjustment is needed) [29].

The unit peak discharge is obtained from the following equation ,which requires the time of concentration (tc) in hours and the initial abstraction /rainfall (la/P) ratio as input[29]:

$$qu = \alpha 10^{c0+c1\log tc+c2(\log tc)^2} \dots\dots\dots\dots\dots (9)$$

7. RESULTS AND DISCUSSION

7.1.Image Classification Results:

The land cover land use map of the study area for 2015 derived from classified Landsat images are shown in Figure 2(a,b) at classification accuracy of (94.58 %) and kappa statistic of 0.93 .It can be observed that the land-cover map derived from the classifications are highly accurate .Analysis of satellite image showed varieties following table (2).

1.Bult-up area

This class is concentrated in the northeast of the basin and is the Iranian city of Ilam, and is concentrated in the center and south of the basin where the city of saleh abad Iranian and Zurbatiyah city in Iraq. This class covers an area (23.79) km 2The proportion (0.83%).

2. Forest

There are forests in the far north-east of the basin, and occupies an area (66.61) km 2 As of (2.32 %) of the basin's total area, and concentrated distribution in the northern part of the basin and oak trees and nut spread in the highlands, which reaches a height of more than (2000) meter above sea level.

3. Grassland or Rangeland

Rangeland historically has been defined as land where the potential natural vegetation is predominantly grasses ,grass like plants, forbs, or shrubs and where natural grazing was an

important influence in its precivilization state[17]. This class covers an area of (298.5)km2 by (10.43 %) is spread in the center of the basin.

4. Agriculture

Agriculture show geometric patterns almost regular visual space, and spread over large parts of northern and central parts of the basin and are sparse in the south of the basin. This class occupies an area of (215.36) km 2 rate (7.52 %).

Mixed Vegetation

This product was spreading from the ground cover in the north and center of the basin and is mixed with farmland. It covers an area of (397.5) km2 by (13.88 %).

5. Barren land

Barren land is land of limited ability to support life .this category includes such areas dry salt flats ,beaches ,bare exposed rock, strip mines ,quarries ,and gravel pits[17]. In the study area the following categories appear within this class:

a. **Alluvial fan deposits***:* It is rough sediments spread at the foot of the mountains is the successive water flooding during fall solely responsible rain for bringing these deposits is assisted by the increasing decline of movable respective regions season, contribute to these deposits Provide some of the necessary raw materials for construction industries such as gravel, sand and spread extraction Factories in the presence areas in Iraqi territory, operating this type of land cover an area (404.71) km 2as of (14.13 %) of the pelvic area.
b. **Brown soils and Chestnut soils**, Covers an area of (305.45) km 2 is a percentage (10.67 %).
c. **Sheet Alluvial fan deposit (dry salt flats):** Covers an area of (675.47) km 2 is a percentage (23.59 %).
d. **Calcareous lithosols (from Sulfurous and Gypsiferous and marls)**: Covers an area of (475.73) km 2 is a percentage (16.62 %).

7.2. HYDROLOGIC MODEL RESULTS:

It has been building a digital spatial database of the study area from (DEM) by using (GIS) accounting for the production of a set of layers that illustrated in Figure 4. Extracted them morphometric characteristics own basin president and secondary basins. Table (2). The land-cover information derived from the analysis of the Landsat images and digital spatial database above were integrated into a hydrologic model as a means of estimating the impacts of the differences in land-cover conditions to the hydrological processes of the watershed, specifically in the generation of runoff and peak discharge forecasting at outlet during rainfall events.

The procedure explained Previously has been used to simulate the flow at outlet of the watershed. The rainfall on October 18, 1994 occurred for24 hrs has been simulated. With the help of this rainfall data cumulative rainfall (P), cumulative abstractions (Ia, and Fa) and effective rainfall (P) have been estimated. Excess rainfall hydrograph values have been calculated by taking the difference of effective rainfall**.** The following presentation and discussion of the most important findings of her study**:**

1. The land cover direct impact on the hydrological Trsak Galal Basin in making curved values high, with an average value of the curved basin 86, and ranged from the high upper and lower values of between 58 and 94. All those high values in excess of the value of the broker to figures curved 50 . In addition to the 69% of the basin area is a high Asmat surfaces where the value of cn for not less than 86, which led to the generation of high runoff in the basin speed Figure 5.a.
2. showed the arithmetic mean of the coefficient value (S) of 41 mm lack the maximum potential of the basin in water retention after the start of the runoff, this value and reflect the gravity of the hydrological situation in the basin, where it is one of the most important function on the speed of the pelvis in response runoff indicators Figure 5.b**.**
3. More than two thirds of the water catchment area are permeability areas low (figures curved in which more than 86 which prevail in regions slope high, with a lack of plant coverage and lower losses leak, shares in high runoff values and speed the flow of water from all over the tub and then moving with regression toward the southern basin, which is a great danger in the lands Iraqi**.**

4. Estimated of the volume of runoff from higher rainstorm fell on the catchment area over a 30 year period, about (171.1) million cubic meters, and estimated volume of runoff from the sub basins 1 and 2 about (62.5) and (100.2) million cubic meters respectively . Table 3.
5. The dimensionless unit hydrograph discussed, has been used to interpolate with the calculated Q/Qp and t/tp values to get discharge (Q) values. The Q values obtained have been multiplied with excess rainfall hydrograph to get discharge at outlet for sub watersheds. Hydrograph for sub watershed 1and 2 is shown in Figure 6 same procedure is applied to get the outlet hydrographs for the Tursaq Galal basin Figure7.The peak discharges, time to peak, base period of the outlet hydrograph of the rainfall events are shown in table 6. From the hydrographs , it is observed that the peak discharge has been found to be 863 m3/sec, 979 m3/sec and 1436 m3/sec and time at which peak discharge occurred at 12th hr, 16.9th hr and 19th hr. for Sub-basins 1 ,2 and The main basin Respectively.

Conclusions

In the present study, the objective is to develop a hydrological model for the simulation of runoff for the event based rainfall of a watershed. Infiltration losses, unit hydrograph and routing are the main model components. Remote sensing and GIS techniques have been used to estimate the spatial variation of the hydrological parameters, which are used as input to the model. SCS curve number and unit hydrograph methods have been used for the estimation of infiltration losses and to synthesis hydrograph respectively. the present work has been applied on the Tursaq Galal basin , Which is located in eastern Iraq, which is extends between Iraq and Iran, between Latitudes (33° 01' 25" -33° 50' 52") north and Longitude (45° 40' 24"- 46° 30' 56") east.

It turned out by searching the Tursaq Galal Basin brings large amounts of water during rainstorms, as much as the volume of water from the rainstorm depth (96) mm 171 million cubic meters and estimated peak discharge (1436) m3/s and time at which peak discharge occurred at 12th hr , posing a major threat to the population and enterprises economic at

outlet of the basin and all areas under its influence. This requires management of the water resource constructing dam at the outlet of each sub-basin.

ACKNOWLEDGMENT

The support of this research by the Iraq- Ministry of higher education and scientific research – University of Thi-Qar & Geography And GIS Department.

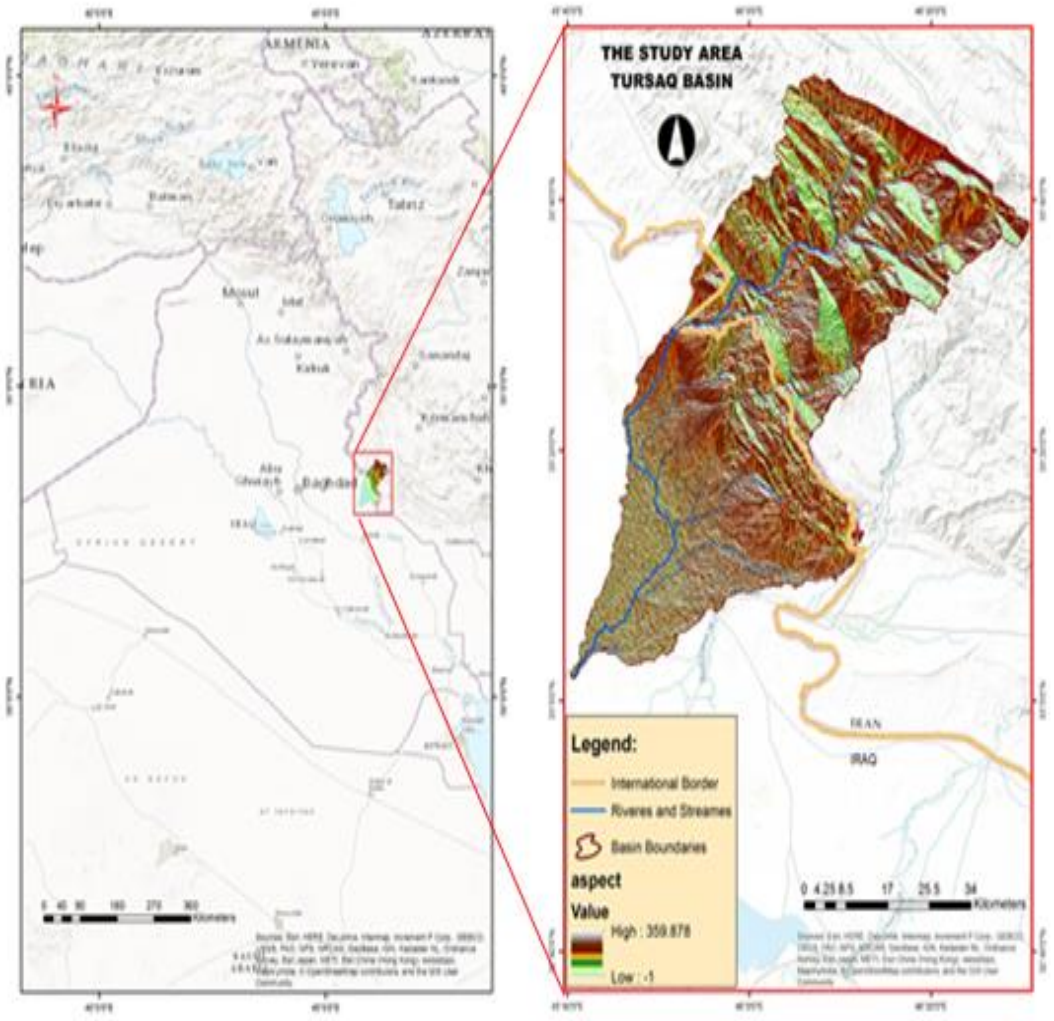


Figure 1: The study area location .

Table (1) Accuracy assessment for supervised classification of Landsat8 (OLI) 2015

Classes	**B**	**F**	**A**	**G**	**MV**	**AF**	**SA**	**BS**	**CL**	**Total**
B	**7**	0	0	0	0	0	0	0	0	7
F	0	**11**	1	0	1	0	0	0	0	13
A	0	0	**18**	0	2	0	0	1	0	21
G	0	0	0	**22**	0	0	0	0	1	23
MV	0	1	0	1	**27**	0	0	0	0	29
AF	0	0	0	0	0	**19**	0	0	0	19
SA	0	0	0	0	0	0	**36**	0	0	36
BS	0	0	0	1	0	0	0	**27**	0	28
CL	0	0	0	0	0	1	1	0	**25**	27
Total	7	12	19	24	30	20	37	28	26	**203**
Overall accuracy =94.58% , Kappa coefficient=0.93										

Note: **B**= Built-up area , **F**= Forest , **A**= Agriculture, **G**= Grassland , **MV**= Mixed Vegetation , **AF**= Alluvial fan deposits , **SA**= Sheet Alluvial fan deposit ,**BS** =Brown soils and Chestnut soils **CL**= Calcareous lithosols (from Sulfurous and Gypsiferous and marls)

Table. 2. AMC conditions.[23]

AMC Class	AMC (mm)	Condition
AMC1	<35	Dry soil but not the wilting point
AMC11	35- 52.5	Average condition.
AMC111	>52.5	Saturated soil; heavy rainfall of lighter rain

Table(3).AMCII -CN values for different land cover /land use types under hydrologic soil groups A,B,C and D which are prevalent in the study area [27].

land use /Land Cover Class	AMCII Curve Number (CN)			
	Soil Group A	Soil Group B	Soil Group C	Soil Group D
Built-up area				94
Forest			70	
Agriculture		78		
Grassland				89
Mixed Vegetation		58	77	
Alluvial fan deposits	77	86		
Sheet Alluvial fan deposit		86	91	
Brown soils and Chestnut soils		86		
Calcareous lithosols (from Sulfurous and Gypsiferous and marls)			91	

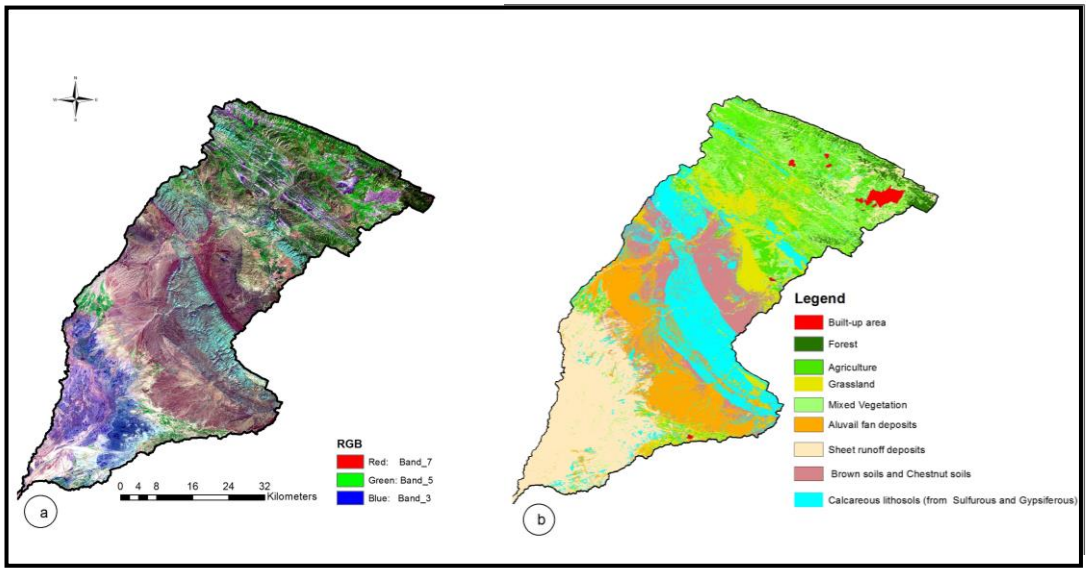


Figure 2. The LULC map derived from the analysis of the Landsat-8 OLI images through Maximum Likelihood classification. (a) Image landsat-8 2015 ; (b) LULC map 2015.

Table (4) Summary of LULC classes in study area statistics for 2015

Land Use Land Cover Class	Area km2	percentage
Built-up area	23.79	0.83
Forest	66.61	2.323
Agriculture	215.36	7.522
Grassland	298.5	10.43
Mixed Vegetation	397.5	13.88
Alluvial fan deposits	404.71	14.135
Sheet Alluvial fan deposit	675.47	23.59
Brown soils and Chestnut soils	305.45	10.67
Calcareous lithosols (from Sulfurous and Gypsiferous	475.73	16.62

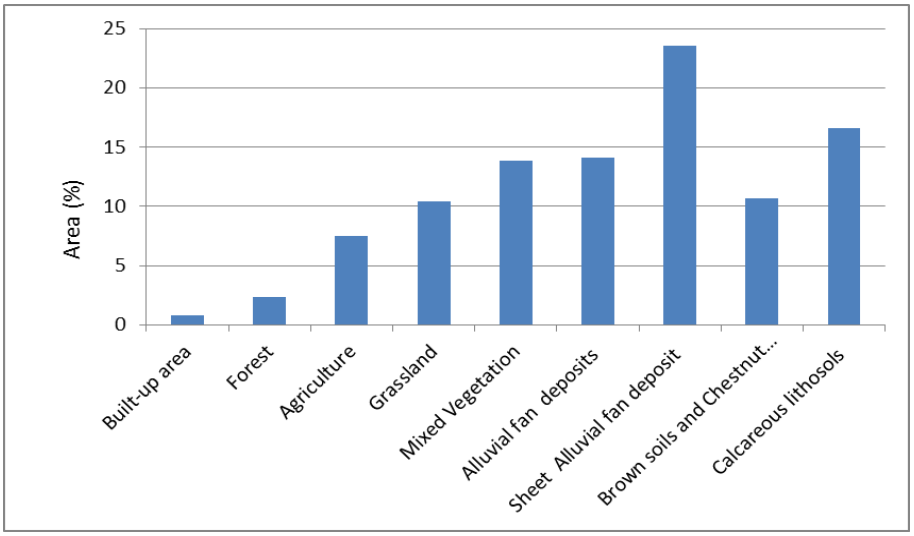


Figure 3. The percentage classes of LULC in the study area 2015

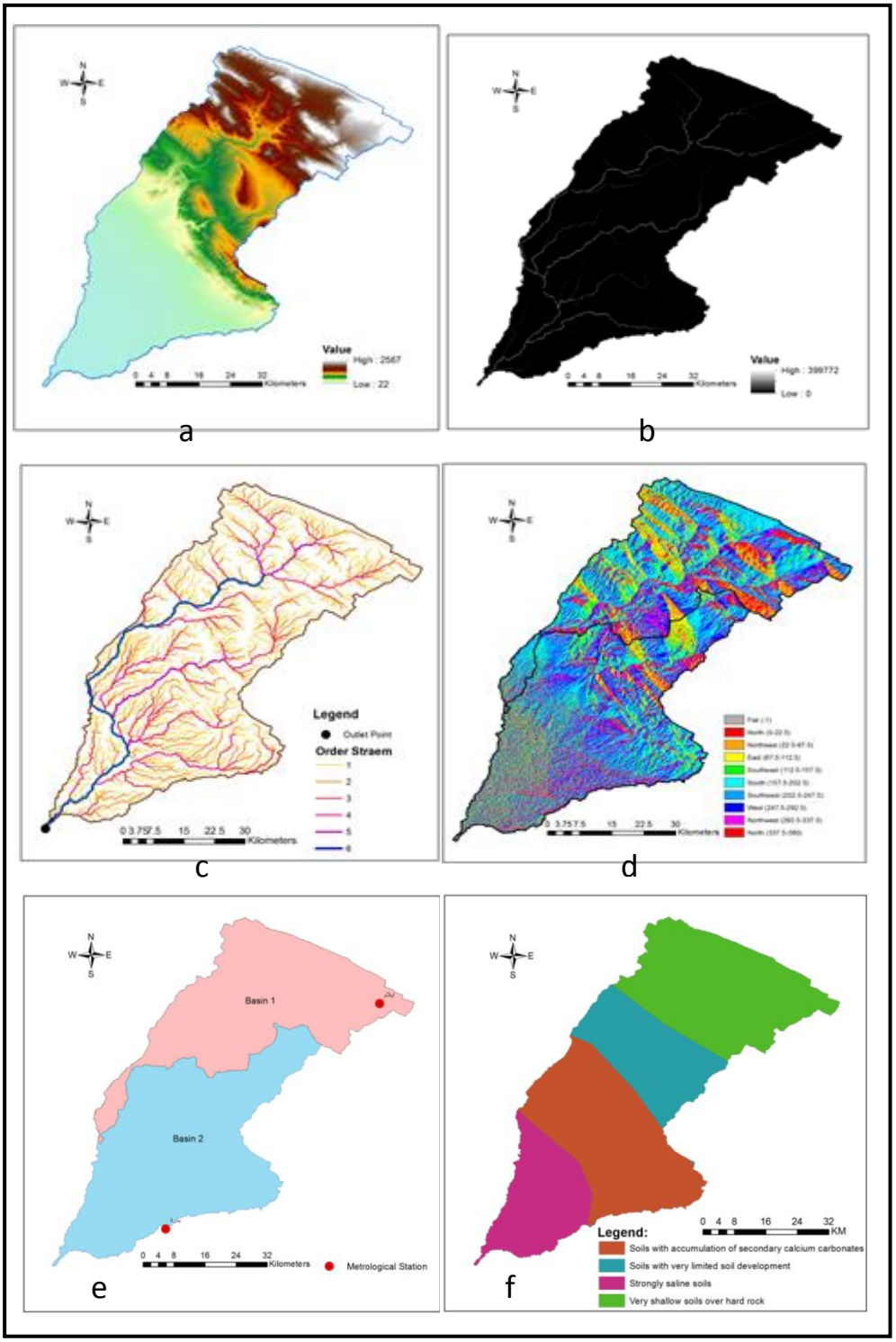


Figure 4. Type of maps represent digital data base for hydrological modeling (a): Digital elevation model (DEM) (b): Flow Direction map (c): Order stream and outlet point (d): Aspect map (e): Sub basin and metrological stations (f): types of soil

Table 5. Morphometric characteristics of some sub-basins main basin

Sub-basin	Area- (km^2)	Length (km)	Slope (%)	Area of pond and swamp (%)	Stream Order
1	1278	61	3.9	0.2	5
2	1585	75	1.92	0.2	5
Tursaq	2863	101	2.47	0.2	6

Table 6. hydrological characteristics of the sub-basins and the main basin

Sub basin	Area- km^2	Metrological Station	Rainfall event (mm)	Curve Number (AMC-II)	S (mm)	Runoff Volume $x10^6\ m^3$	Tp (h)	Qp M3/s	Tc (h)
1	1278	ILAM	96.2	80.79	60.39	62.587	12.2	863	18.12
2	1585	BADRAH	96.1	87.56	36.08	100.192	16.9	979	25.40
Tursaq	2863	Average Ilam and Badrah	96.15	86	41.34	171.103	19.2	1436	28.86

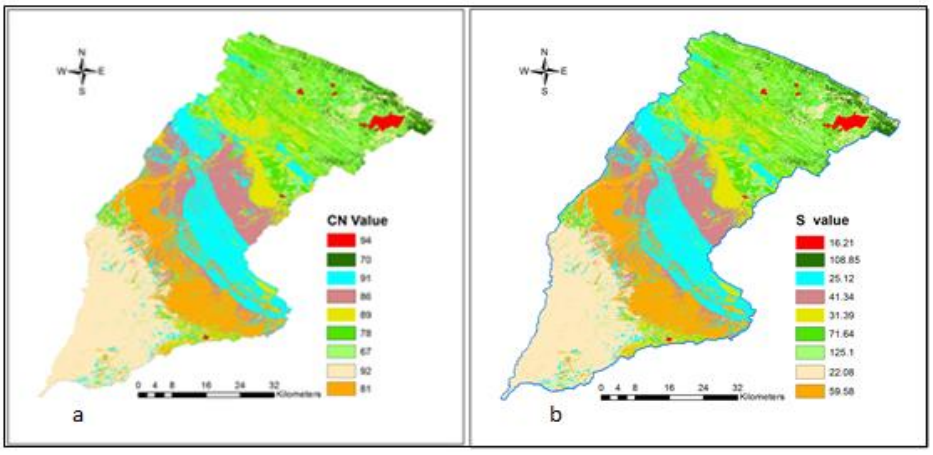


Figure 5. The maps derived from the analysis of the LULC map (a) Curve Number (CN) value (b) Potential Maximum Retention (S) value

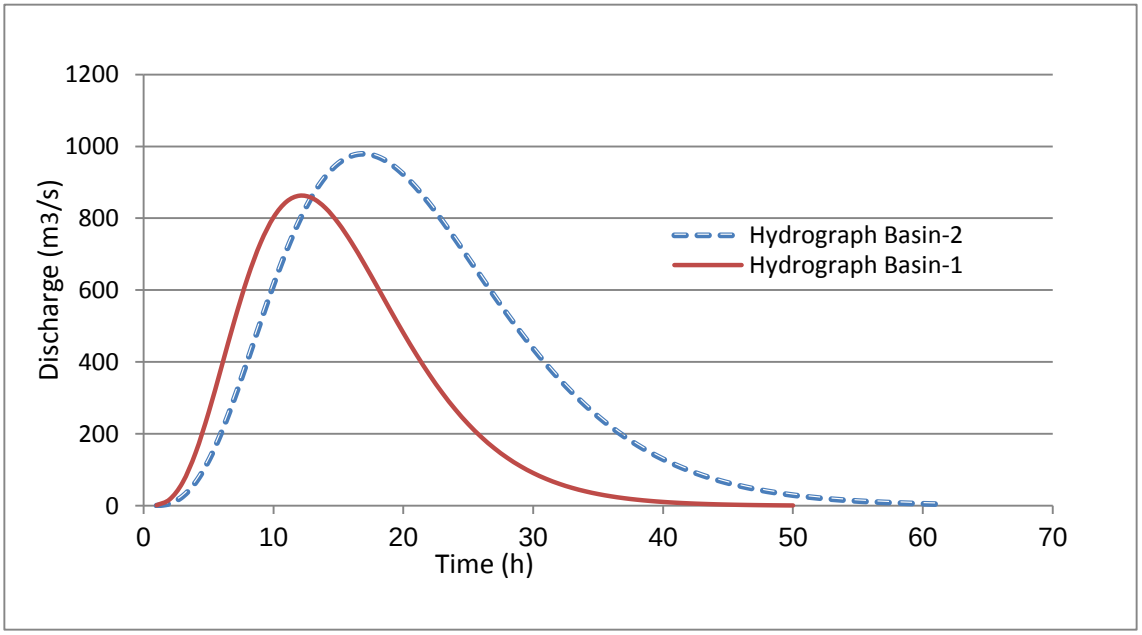


Figure 6. Hydrograph at Outlet of Sub basins for Rainfall Event of August 29, 2008

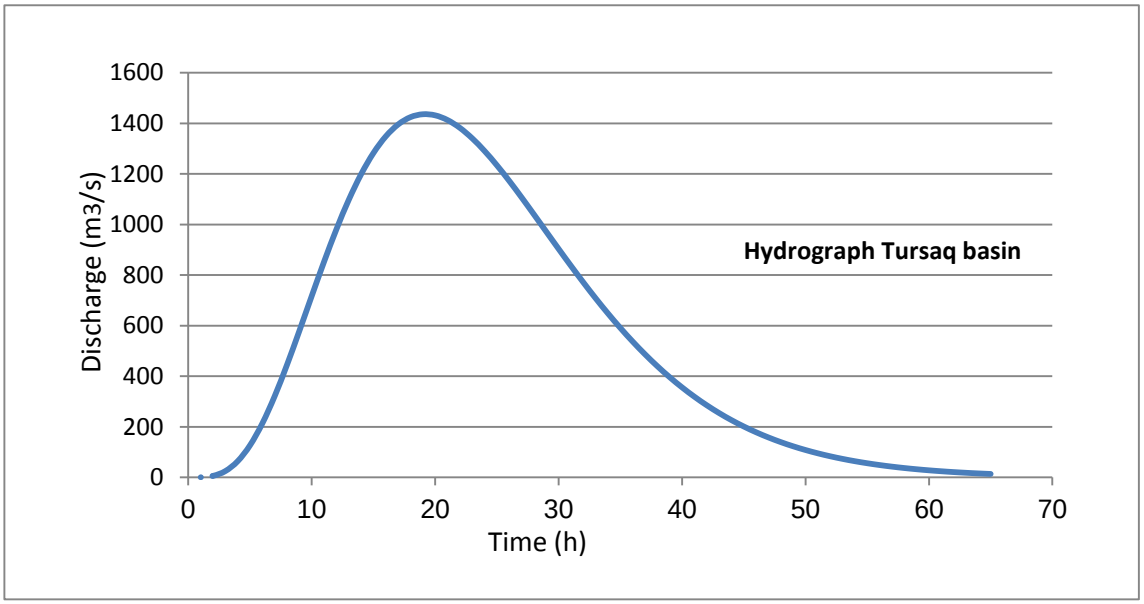


Figure 7. Hydrograph at Outlet of Tursaq Galal Basin for Rainfall Event of October 18, 1994

REFERENCES

1. Engman, E. T. and Gurney, R. J. (1991) Remote Sensing in Hydrology, Chapman and Hall, London, 225 p.
2. Schultz, G.A. (1988) remote sensing in hydrology, Journal of Hydrology, No. 100, pp. 239-265.
3. Kite, G.W. (1991) A watershed model using satellite data applied to a mountain basin in Canada, Journal of Hydrology, No. 128: 157-169.
4. Metrological data(1985-2015) for Ilam station, Iran.
5. Metrological data(1994-2015) for Badra station, Iraq.
6. U.S. Geological Survey, 2013, Landsat—A Global Land-Imaging Mission. http://remotesensing.usgs.gov.
7. Digital elevation model (DEM) with resolution 30m download from website of aster GDEM (http://gdem.ersdac.jspacesystems.or.jp/search.jsp)
8. Geological survey of Iran, Soil map of Ilam, scale 1:500000 in digital format.
9. Geological survey of Iran, geology map of Ilam (2004) , Iran, , scale 1:5000001:500000 in digital format.
10. William K. Pratt (2007), Digital Image Processing , A John Wiley & Sons, Inc., Publication, USA.
11. Jay Gao(2012), Digital Analysis of Remotely Sensed Imagery, Mc Graw Hill, New York .
12. Campbell, J.B. (1996). Introduction to Remote Sensing. Taylor & Francis, London.
13. Steven M. DE Jong and Freek D. Van Der Meer (2004), Remote Sensing Image Analysis : Including The Spatial Domain , Kluwer Academic Publishers, NEW YORK.
14. J.R. Anderson, and others,(1976) , Land use and Land cover classification system for use with Remote sensing Data, U. S. Geological survey professional, NEW YORK.
15. Barson, M.M. (1999). Workshop on Land Use Management Mapping. Report to the National Land and Water Resources Audit. Bureau of Rural Sciences, Canberra.
16. Ramachandra.T. V and Kumar(2004) . Uttam Geographic Resources Decision Support System for land use land cover dynamics analysis, Proceedings of the FOSS/GRASS Users

    Conference - Bangkok, Thailand, 12-14 September 2004, p.2.
17. Lillesand T.M. & Kiefer, R.W. (2000) Remote Sensing and Image Interpretation. John Wiley & Sons, New York, 724 pp.

18. Jay Gao(2012), Digital Analysis of Remotely Sensed Imagery, Mc Graw Hill, New York.
19. Janaza F. J., (1993) ,Manual of Remote Sensing , Theory Instruments & Techniques, American Society of Photogrammetry, Falls Church, Virginia, Vol. 1 .
20. Jensen, J.R. (2004). Introduction to Digital Image Processing: A Remote Sensing Perspective. Practice Hall, New Jersey.
21. Russell G. Congalton And Kass Green (2009), Assessing the Accuracy of Remotely Sensed Data, Taylor & Francis Group, LLC, New York.
22. Watershed modeling system (2009) ,user manual,.
23. USDA-SCS,(1985), Natural Engineering Handbook, section 4. Department of Agriculture, USA .
24. Ponce, V.M.; Hawkins(1996), R.H. Runoff curve number: Has it reached maturity J. Hydrol. Eng., 11-19.
25. USDA-TR55, (1986), Urban Hydrology for Small Watersheds, Department of Agriculture, USA.
26. David A. Chin(2004) , Water-Resources Engineering, Second Edition. New York.
27. Taylor & Francis (1982), The antecedent soil moisture condition of the curve number procedure, Hydrological Sciences Journal, Duchy of Luxembourg.
28. H. Raghunath (2006), Hydrology: Principles, Analysis, and Design, New Age International Ltd., New Delhi, India .
29. U.S. Department of Transportation National Highway Institute(2002), Highway Hydrology , Hydraulic Design Series No. 2, Second Edition.
30. Curtis Weaver, J., (2003), Methods for Estimating Peak Discharges and Unit Hydrographs for Streams in the City of Charlotte and Mecklenburg County, North Carolina. Water Resources Investigations Report 03–4108, p55.
31. Z. Sen(2008) ,Wadi hydrology , CRC Press, New York.